UC Irvine
UC Irvine Previously Published Works

Title

A Test of Climate, Sun, and Culture Relationships from an 1810-Year Chinese Cave Record

Permalink

https://escholarship.org/uc/item/7490451m

Journal

Science, 322(5903)

ISSN

0036-8075

Authors

Zhang, Pingzhong
Cheng, Hai
Edwards, R Lawrence
et al.

Publication Date

2008-11-07

DOI

10.1126/science.1163965

Copyright Information

Peer reviewed

A Test of Climate, Sun, and Culture Relationships from an 1810-Year Chinese Cave Record

Pingzhong Zhang,[1] Hai Cheng,[2]* R. Lawrence Edwards,[2] Fahu Chen,[1] Yongjin Wang,[3] Xunlin Yang,[1] Jian Liu,[4] Ming Tan,[5] Xianfeng Wang,[2] Jinghua Liu,[1] Chunlei An,[1] Zhibo Dai,[1] Jing Zhou,[1] Dezhong Zhang,[1] Jihong Jia,[1] Liya Jin,[1] Kathleen R. Johnson[6]

A record from Wanxiang Cave, China, characterizes Asian Monsoon (AM) history over the past 1810 years. The summer monsoon correlates with solar variability, Northern Hemisphere and Chinese temperature, Alpine glacial retreat, and Chinese cultural changes. It was generally strong during Europe's Medieval Warm Period and weak during Europe's Little Ice Age, as well as during the final decades of the Tang, Yuan, and Ming Dynasties, all times that were characterized by popular unrest. It was strong during the first several decades of the Northern Song Dynasty, a period of increased rice cultivation and dramatic population increase. The sign of the correlation between the AM and temperature switches around 1960, suggesting that anthropogenic forcing superseded natural forcing as the major driver of AM changes in the late 20th century.

Interest in Asian Monsoon (AM) variability is high because of tropical ocean/atmosphere interactions involving the AM and the AM's role in transporting large quantities of heat and water vapor to the most-populated regions of the world. Recent cave climate studies have reconstructed the monsoon's history back thousands (1) to hundreds of thousands of years (2). However, we still do not know, in detail, how late Holocene AM changes relate to solar activity, climate in other regions, anthropogenic forcing, and cultural changes, mainly because of age uncertainties and the insufficient resolution of existing records. We identified an unusual stalagmite sample from Wanxiang Cave, China, that is ideally suited to mitigate these problems. High growth rate, high uranium concentrations, and low thorium concentrations allow high oxygen isotope resolution and high-precision ^{230}Th ages. The cave is located on the fringes of the area currently affected by the summer monsoon and is thus sensitive to and integrates broad changes in the monsoon.

Wanxiang Cave (33°19'N, 105°00'E, 1200 m above sea level) is between the Qinghai-Tibetan Plateau and the Chinese Loess Plateau in Wudu County, Gansu Province, China (fig. S1). Cave and mean annual temperatures are ~11°C. The region is semi-arid (fig. S1), with annual precipitation of 480 mm, 80% of which falls be-

tween May and September. During winter, the Siberian-Mongolian High and westerly winds maintain cold and dry conditions and carry airborne dust to the site. In May 2003, about 1 km from the cave entrance, we collected a 118-mm-long stalagmite (WX42B), which had grown continuously from 190 to 2003 A.D. (table S1 and fig. S2). The record was established with 703 δ^{18}O analyses with an average resolution of 2.5 years, errors in ^{230}Th age of <5 years (Fig. 1), and errors associated with subsampling position of <15 years [materials and methods in supporting online material (SOM) and table S2]. A Hendy test (3) and other lines of reasoning suggest that the calcite was deposited in isotopic equilibrium and that the δ^{18}O signal largely anticorrelates with precipitation (materials and methods in SOM and figs. S3 and S4). Comparisons with existing cave records from China are difficult because of differing oxygen isotope resolution and dating uncertainties (fig. S5). However, a recent precipitation record [(4), from historical documents] from Longxi (~150 km to the north) exhibits close similarity to the cave record (Fig. 2A), further supporting the precipitation/cave δ^{18}O relationship.

The Wanxiang record, with a δ^{18}O range of ~1.3 per mil (‰) (Fig. 1), exhibits a series of centennial to multicentennial fluctuations broadly similar to those documented in Northern Hemisphere (NH) temperature reconstructions, including the Current Warm Period (CWP), Little Ice Age (LIA), Medieval Warm Period (MWP), and Dark Age Cold Period (DACP) (5–8). Between 190 and 530 A.D. (the end of the Han Dynasty and most of the Era of Disunity), the summer monsoon is moderately strong, but with substantial decadal- to centennial-scale fluctuation. From 530 to 850 A.D. (the end of the Era of Disunity, the Sui Dynasty, and most of the Tang Dynasty), the AM generally declines, then decreases sharply to a relative minimum at 860 A.D. It maintains low values until another sharp

drop between 910 and 930 A.D., then rises dramatically over 60 years to a maximum at around 980 A.D., maintaining high values until 1020 A.D. We term the weak monsoon period between 850 and 940 A.D. the Late Tang Weak Monsoon Period (LTWMP; the last six decades of the Tang Dynasty and the first three decades of the Five Dynasties and Ten Kingdoms period). Similarly, we refer to the ensuing strong monsoon peak (960 to 1020 A.D.) as the Northern Song Strong Monsoon Period (NSSMP; the first six decades of the Northern Song Dynasty). After 1020 A.D., the monsoon fluctuates considerably but is generally strong until a sharp drop between 1340 and 1360 A.D.: the mid–14th-century monsoon weakening. It maintains weak values, with substantial fluctuation, until a sharp increase between 1850 and 1880 A.D.: the late–19th-century monsoon strengthening. Punctuating the generally weak monsoon of the 14th to 19th centuries are unusually weak periods from 1350 to 1380 A.D. (the Late Yuan Weak Monsoon Period, LYWMP) and from 1580 to 1640 A.D. (the Late Ming Weak Monsoon Period, LMWMP). The last major feature of the monsoon is a distinct weakening at the end of the 20th century (1960 to 2000 A.D.).

A 9th-century dry period has been invoked as contributing to the decline of the Tang Dynasty (9) and the Mayans in Mesoamerica (10–12), an idea that has generated substantial discussion (13). The timing of the LTWMP is consistent with this idea, particularly as the Tang was in decline in its final decades. Because the LTWMP continued beyond the Tang, it may have also contributed to the lack of unity during the Five Dynasties and Ten Kingdoms period. Moreover, the ensuing NSSMP may have contributed to the rapid increase in rice cultivation, the dramatic increase in population, and the general stability at the beginning of the Northern Song Dynasty (14). Furthermore, the end of the Yuan and the end of the Ming are both characterized by unusually weak summer monsoons (the LYWMP and the LMWMP), suggesting a link between climate and the demise of these dynasties as well. Whereas other factors would certainly have affected these chapters of Chinese cultural history, our correlations suggest that climate played a key role.

The relationship between the AM and the Swiss record of Alpine glaciation (8), portions of which are dated to the year, is clear, with times of weak summer AM correlating with Alpine advances (Fig. 2B). The Swiss record captures a 9th-century glacial advance (that correlates with the LTWMP), followed by glacial retreat to high elevations for much of the late 9th to early 14th centuries (corresponding broadly to the MWP and the generally strong AM between 950 and 1340 A.D.). A prominent advance correlates with the mid–14th-century monsoon weakening and the LYWMP, the first of three LIA advances that correlate with a generally weak AM. The second and largest, centered at about 1600 A.D., corre-
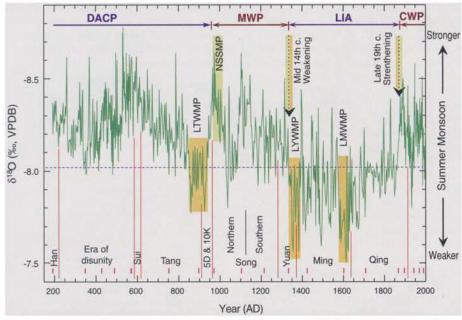
[1]Key Laboratory of Western China's Environmental Systems (Ministry of Education), College of Earth and Environment Sciences, Lanzhou University, Lanzhou 730000, China. [2]Department of Geology and Geophysics, University of Minnesota, Minneapolis, MN 55455, USA. [3]College of Geography Science, Nanjing Normal University, Nanjing 210097, China. [4]Nanjing Institute of Geography and Limnology, Chinese Academy of Sciences, Nanjing 210008, China. [5]Institute of Geology and Geophysics, Chinese Academy of Sciences, Beijing 100029, China. [6]Department of Earth System Science, University of California, Irvine, Irvine, CA 92697, USA.

*To whom correspondences should be addressed. E-mail: cheng021@umn.edu

Fig. 1. The WX42B δ¹⁸O record. Pink vertical bars show locations of ^{230}Th dates, with errors of ±1 to ±5 years. The three yellow vertical bars denote the LTWMP, LYWMP, and LMWMP; the shaded green bar denotes the NSSMP. Chinese dynasties are indicated, as are the mid–14th-century monsoon weakening and the late–19th-century monsoon strengthening. 5D & 10K stands for the Five Dynasties and Ten Kingdoms period.
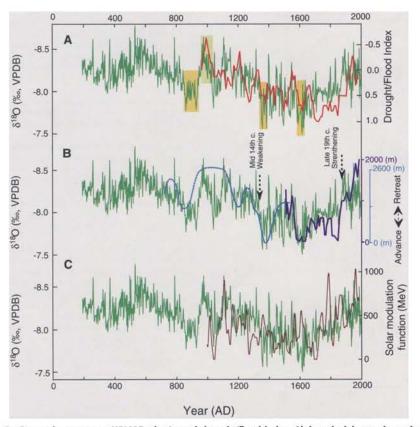

Fig. 2. Comparisons among WX42B, the Longxi drought/flood index, Alpine glacial records, and solar irradiance. The δ¹⁸O time series of WX42B is in dark green. Yellow vertical bars are as in Fig. 1. (**A**) Reconstructed drought/flood index from Longxi, ~150 km north of Wanxiang Cave [red (4)]. (**B**) Swiss Alpine glaciation (dark blue, Gorner glacier; light blue, Lower Grindelwald glacier) (8). Portions are dated to the year; the dashed portion is dated less precisely (with ¹⁴C dates). (**C**) Solar irradiance from ¹⁰Be and ¹⁴C records [brown (22)]. See also fig. S8.

lates with the LMWMP. A retreat, marking the end of the LIA, correlates well with the late–19th-century strengthening of the AM, an event that also correlates with glacial retreat in many localities worldwide and with abrupt freshening and cooling of surface waters in the southwest tropical Pacific (15). These correlations demonstrate that the link between North Atlantic/European and East Asian climate, established deeper in time (1, 16), continues into the latest Holocene (except for the end of the 20th century).

The geographic imprint of the LTWMP extends well beyond the Alps, probably including a large portion of the NH low and mid-latitudes. In addition to the aforementioned dry events recorded in Lake Huguang Maar (9), Mesoamerica (10–12), and the Cariaco (17), as well as the Alpine glacial advance (8), this event correlates with dry events recorded on Barbados (18), in southern France (19), and in southeastern Minnesota (20). The latter two examples correlate with the LTWMP at very high temporal precision. The LTWMP's broad NH footprint supports the idea of a southerly shift in the Intertropical Convergence Zone (10), with teleconnections to higher northern latitude sites (fig. S6).
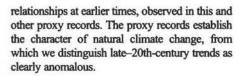
Based on speleothem records with chronologies tuned to ¹⁴C records (1, 21), solar forcing has been identified as one factor affecting the AM. Our record provides a rigorous test of this idea (tables S1 and S2). Spectral analysis yields significant periods at 170, 10.5, and 5 to 6 years, with the 10.5-year period corresponding to the Schwabe sunspot cycle (fig. S7). The AM also has correlations to solar irradiance as inferred from ¹⁴C and ¹⁰Be records (22) [correlation coefficient (r) = –0.33, n = 345 data points for the past millennium, Fig. 2C and fig. S8]. These observations support the idea that solar forcing played a role in driving AM changes during the past two millennia (1, 5–7, 21). However, it is clear from this and other studies (1, 5–7, 21) that other factors control much of the variability in the AM. For example, one of the most prominent features in our record, the mid–14th-century monsoon weakening, takes place the better part of a century after a major inferred drop in solar intensity (22) (Fig. 2C) and is therefore not likely to be the result of that solar shift.

Summer AM precipitation is driven by the thermal contrast between Asia and the tropical Indo-Pacific and therefore should be linked to regional temperature change (16). Based on an ECHO-G climate model simulation (SOM), we modeled Chinese air temperature for the past millennium, with results that were broadly consistent with our record (r = –0.46 and n = 345 data points), particularly with regard to centennial and multicentennial time scales and with regard to the distinct double peak in both model output and record during the MWP (Fig. 3A). Because the ECHO-G model includes solar (and volcanic) forcing, this broad agreement further substantiates the view that solar forcing plays a role in AM variability.

Our record has substantial similarities to NH temperature reconstructions (5–7) (Fig. 3), with notable differences: (i) The AM peak at 550 A.D. is higher than correlative temperature anomalies (Fig. 3, C and D), and (ii) the timing of the onset (950 A.D.) and end (1340 A.D.) of the strong AM at about the time of the MWP differ from those of the NH temperature anomaly [~890 to 1170 A.D. (23)]. In both cases, our record follows solar variability more closely than NH temperature. Solar irradiance reached its highest value in the past two millennia (fig. S8) at the same time as the 550 A.D. AM peak. At about the time of the MWP, the AM and solar irradiance peaks (24) have similar timing. These observations suggest that the AM and Chinese temperature respond more strongly to solar irradiance than does mean NH temperature.

Our record shows general AM weakening over the past half century, with much of the change taking place in the past two decades, which is consistent with other AM indices (fig. S9) and anticorrelating with rising NH temperature (5–7). This late-20th-century anticorrelation is distinctly anomalous as compared to earlier times, which are characterized by millennial- and centennial-scale correlation between NH temperature and the AM (Fig. 2), as well as similar

correlations between the AM and North Atlantic temperature much deeper in time (2, 16). This anomaly suggests that the dominant forcing of AM variability changed from natural to anthropogenic around 1960 (25–27). Possible mechanisms include differences in the nature of solar versus greenhouse forcing, the effect of anthropogenic black carbon on the AM, and/or the effect of anthropogenic sulfate aerosols. Solar forcing is more seasonally and spatially heterogeneous than greenhouse gas forcing and thus is more likely to induce feedbacks involving temperature gradient–driven circulation such as the AM (25). Models have also shown that lower-troposphere cooling coupled with mid- and upper-troposphere heating caused by black carbon could reduce East Asian Monsoon precipitation as observed (28). Finally, models also suggest that the indirect effect of differential anthropogenic sulfate aerosol loading shifts tropical rainfall southward (29), plausibly weakening the monsoon as observed. Thus, variability in late–20th-century precipitation and temperature in the region is probably caused, in large part, by both anthropogenic greenhouse gases and aerosols. In reaching this conclusion, the key observation was not our late–20th-century trend, which is also observed in instrumental records, but rather the

relationships at earlier times, observed in this and other proxy records. The proxy records establish the character of natural climate change, from which we distinguish late–20th-century trends as clearly anomalous.

Reference and Notes

1. Y. J. Wang et al., Science **308**, 1090 (2005).
2. Y. J. Wang et al., Nature **451**, 854 (2008).
3. C. H. Hendy, Geochim. Cosmochim. Acta **35**, 801 (1971).
4. L. C. Tan, Y. J. Cai, L. Yi, Z. S. An, L. Ai, Clim. Past **4**, 19 (2008).
5. J. Esper, E. R. Cook, F. H. Schweingruber, Science **295**, 2250 (2002).
6. M. E. Mann, P. D. Jones, Geophys. Res. Lett. **30**, 1820 (2003).
7. A. Moberg, D. M. Sonechkin, K. Holmgren, N. M. Datsenko, W. Karlén, Nature **433**, 613 (2005).
8. H. Holzhauser, M. Magny, H. J. Zumbuhl, Holocene **15**, 789 (2005).
9. G. Yancheva et al., Nature **445**, 74 (2007).
10. J. W. Webster et al., Palaeogeogr. Palaeoclimatol. Palaeoecol. **250**, 1 (2007).
11. D. A. Hodell, M. Brenner, J. H. Curtis, T. Guilderson, Science **292**, 1367 (2001).
12. J. H. Curtis, D. A. Hodell, M. Brenner, Quat. Res. **46**, 37 (1996).
13. D. E. Zhang, L. H. Lu, Nature **450**, 10.1038/nature06338 (2007).
14. J. A. G. Roberts, A History of China (Palgrave Macmillan, ed. 2, New York, 2006).
15. E. J. Hendy et al., Science **295**, 1511 (2002).
16. H. Cheng et al., Geology **34**, 217 (2006).
17. G. H. Haug, K. A. Hughen, D. M. Sigman, L. C. Peterson, U. Rohl, Science **293**, 1304 (2001).
18. J. L. Banner, M. Musgrove, Y. Asmerom, R. L. Edwards, J. A. Hoff, Geology **24**, 1049 (1996).
19. E. M. McMillan, I. J. Fairchild, A. Borsato, F. McDermott, J. Quat. Sci. **20**, 423 (2005).
20. S. Dasgupta, thesis, Univ. of Minnesota, Minneapolis, MN (2008).
21. U. Neff et al., Nature **411**, 290 (2001).
22. R. Muscheler et al., Quat. Sci. Rev. **26**, 82 (2007).
23. T. J. Osborn, K. R. Briffa, Science **311**, 841 (2006).
24. E. Bard, M. Frank, Earth Planet. Sci. Lett. **248**, 1 (2006).
25. G. A. Meehl, W. M. Washington, T. M. L. Wigley, J. M. Arblaster, A. Dai, J. Clim. **16**, 426 (2003).
26. C. M. Ammann, F. Joos, D. S. Schimel, B. L. Otto-Bliesner, R. A. Tomas, Proc. Natl. Acad. Sci. U.S.A. **104**, 3713 (2007).
27. M. Lockwood, C. Fröhlich, Proc. R. Soc. London Ser. A **463**, 2086 (2007).
28. K. M. Lau, M. K. Kim, K. M. Kim, Clim. Dyn. **26**, 855 (2006).
29. L. D. Rotstayn, U. Lohmann, J. Clim. **15**, 2103 (2002).
30. We thank R. S. Bradley for his comments that improved this manuscript considerably and W. S. Broecker and the late G. Comer for their support of our work. This work was supported by the National Science Foundations of the United States (grant NSF ESH 0502535 to R.L.E. and H.C.) and China (grants NSFC 40421101, 40471137, and 40721061 to P.Z. and 40225007 to Y.J.W. and H.C.), the Gary Comer Science and Education Foundation (grants CC8 and CP41 to R.L.E.), the Ministry of Science and Technology of China (grant 2006CB400503 to M.T.), and the Chinese Academy of Sciences (grant KZCX2-YW-316 to M.T.).
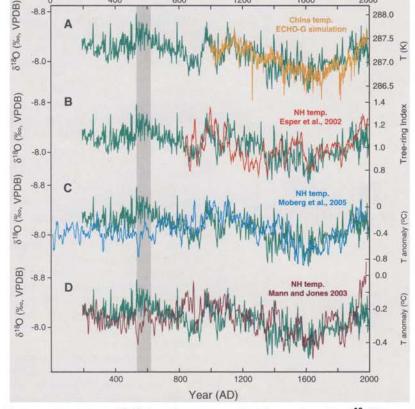
Fig. 3. Comparison between WX42B and proxy or modeled temperature. The $\delta^{18}O$ time series of WX42B is in dark green. (**A**) Modeled Chinese temperature from an ECHO-G model simulation (orange). (**B** to **D**) NH temperature reconstructions from proxy records: (B) red curve (5), (C) blue curve [smoothed with a 10-year running mean (7)], and (D) dark brown curve (6). The gray vertical bar depicts a time characterized by a discrepancy between the AM record and NH temperature reconstructions, as discussed in the text.